Supplementary Information

Hierarchical $CoS_2/Ni_3S_2/CoNiO_x$ Nanorods with Favorable Stability at 1 A cm^{-2} for Electrocatalytic Water Oxidation

Husileng Lee,[a] Xiujuan Wu,*[a] Qilun Ye,[a] Xingqiang Wu,[a] Xiaoxiao Wang,[a] Yimeng Zhao,[a] Licheng Sun* [a,b,c]

[a] *State Key Laboratory of Fine Chemicals, DUT-KTH Joint Education and Research Center on Molecular Devices, Dalian University of Technology (DUT), 116024 Dalian, China*

[b] *Department of Chemistry, School of Chemical Science and Engineering, KTH Royal Institute of Technology, 10044 Stockholm, Sweden*

[c] *Institute for Energy Science and Technology, Dalian University of Technology (DUT), Dalian 116024, China.*

Corresponding Author

Xiujuan Wu, email: wuxiujuan2003@dlut.edu.cn.

Licheng Sun, email: lichengs@kth.se

General materials and instruments

CoNi foam was purchased from Kunshan Jijinsheng Electronic technology Co. Ltd. 5 wt. % Nafion solution and Thiourea (98%) were purchased from Sigma-Aldrich or TCI. RuO_2 (95%) and KOH (99.99%) were purchased from Alfa. Ni powder and Co powder were purchased from the Tianjin Damao reagent factory (>99.5%). Other chemical reagents were analytical pure and used without further purification. Ultra-pure water (18.2 MΩ cm) for all the reactions or measurements was obtained from a Milli-Q system (Millipore, Direct-Q 3 UV).

SEM images and EDX spectra were obtained by using Nova NanoSEM 450 equipment. Images were obtained with an acceleration voltage of 3 kV and EDX Electronic spectra were obtained with an acceleration voltage of 20 kV. TEM and HRTEM images were taken on (FEI TF30) TEM system operating at 300 kV equipped with EDX system. The content of the catalyst was quantified by an inductively coupled plasma optical emission (ICP-OES) spectrometer (Optima 2000 DV, America PerkinElmer Corp.) after sonicated the catalyst in ethanol for 60 min. X-ray photoelectron spectroscopy (XPS) measurement was performed on a Thermo Scientific ESCALAB 250 instrument using 200 W Kα radiation. The binding energy (BE) was calibrated with respect to the C 1s level 284.6 eV of adventitious carbon. Raman spectra of the catalyst were recorded using a confocal Raman microscope (DXR Raman Microscope, Thermo Scientific). Spectra were acquired with 1 mW of 532 nm laser excitation at the sample surface. X-ray diffraction (XRD) analysis was conducted on Rigaku D/Max 2400 (Japan) using Cu Kα radiation (λ = 0.1541 nm) at a scanning rate of 5°/min in the 2θ range of 10 - 80°. The Brunauer–Emmett–Teller (BET) surface area and porous structure were measured using a BELSORP-max instrument from Ar adsorption and desorption isotherms at 77 K.

Preparation of the $CoS_2/Ni_3S_2/CoNiO_x$

A piece of CoNi foam (2 cm x 2 cm) was cleaned ultrasonically first with 2 M HCl, DI water and acetone for 30 min in each. The cleaned CoNi foam was put into a 50 mL Teflon-lined stainless autoclave containing 35 mL of 2.89 mM thiourea solution. The autoclave was sealed and maintained at 120 °C for 12 h. The resulting material was washed with ethanol three times and dried in an oven at 60 °C, giving the catalyst.

Preparation of Ni_3S_2 NP and CoS_2 NP

Ni_3S_2 NP and CoS_2 NP were prepared by hydrothermal reaction according to literature reported method. Briefly, 60 mg Ni powder or Co powder was put into 20 mL 2.63 mM thiourea solution and stirred vigorously for about 30 min. Then, the solution was poured into a 50 mL Teflon-lined stainless autoclave and the autoclave was sealed at 120 °C for 12 h. Finally, the resulting material was washed with ethanol three times and dried in an oven at 60 °C, giving the aimed product.

Preparation of other working electrodes

5 mg Ni_3S_2-NP, CoS_2-NP, and RuO_2 powder were dispersed in 0.98 mL mixture of isopropyl alcohol and ultrapure water (1:1) and mixed with 20 μL 5 wt. % Nafion solution. Then, the mixture was sonicated for 0.5 h to form homogeneous ink. A definite volume of the ink was drop-casted on the surface of the 1 cm^{-2} CoNi foam to form a catalyst film and dried at room temperature (loading amount ≈ 1.25 mg/cm^2).

Electrochemistry

All electrochemical experiments were carried out using a CHI 660E Electrochemical Analyzer at room temperature. In a typical test, an undivided three-electrode configuration with 20 mL electrolyte was used in the experiments. A catalyst-coated CoNi foam was used as a working electrode (WE), and the

geometric area of WE was maintained as 1 cm^2. Other samples for comparison, namely Ni_3S_2-NP, CoS_2-NP, and RuO_2, were sealed with 5% Nafion solution on bare CoNi foam (loading amount: 1.25 mg cm^{-1}). Hg/HgO (1 M KOH) was used as a reference electrode (RE) and Pt wire was used as a counter electrode (CE). The reference electrode was calibrated by using redox couple $[Ru(bpy)_3]^{3+}/[Ru(bpy)_3]^{2+}$ ($E_{1/2}$ = 1.26 V *vs.* NHE) as a standard. All potentials reported in this work were converted to the RHE reference scale using E (RHE) = E (RE) + 0.059 pH + 0.112 V. All LSV tests in this text, the resistance was corrected by 85% *i*R compensation function available on the CHI potentiostats.

The polarization curves were obtained by linear sweep voltammetry (LSV) tests conducted in 1.0 M KOH, at a scan rate of 5 mV s^{-1} and with 85% *iR* compensation. Chronopotentiometry (CP) curves were recorded at a constant potential without iR-compensation. Tafel plots were obtained by linear fitting the Faradic region of LSV curves mentioned above. Electrochemical impedance spectroscopy (EIS) of catalysts and other samples were recorded under a bias of 1.53 V over a frequency of 0.1 Hz to 1 MHz with an amplitude potential of 5 mV.

For testing the durability of catalyst, an undivided and tightly sealed (avoid evaporation of water) three-electrode configuration with 40 mL 30% KOH solution was used. In the test, 0.25 cm^2 catalyst-coated CoNi foam, Hg/HgO (1 M KOH) and Pt wire were used as WE, RE and CE, respectively.

For Faraday efficiency evaluation, we use a single compartment gas-tight cell equipped with the three-electrode system described above. In the system, catalyst film (immersed geometric area: 1 cm^2) as the working electrode, Hg/HgO (1 M KOH) and Pt mesh as the reference electrode and counter electrode, respectively. Prior to measurement, the solution was degassed by bubbling Ar for 2 h. The experiment was carried out at 1.48 V *vs.* RHE without *iR* compensation in 1.0 M pH 13.6 KOH solution for 2 h. During the bulk electrolysis, the amount of evolved oxygen in the headspace was taken each 20 min and quantified by

GC (GC 7890T instrument equipped with a thermal conductive detector). The Faradaic efficiency can be calculated as Faradaic efficiency = $4F \times nO_2/Q$, where Q is the total amount of charge passed through the cell under the constant potential, F is the Faraday constant (96485 C mol^{-1}).

To measure C_{dl} of prepared films, CVs were swept between 0.814 V ~ 0.914 V in 1.0 M KOH at different scan rates (20, 40, 60, 80, 100, 120, and 140 mV s^{-1}). The C_{dl} values were estimated by plotting $\Delta J = J_a - J_c$ at 0.864 V against scan rates. The slopes were twice of the C_{dl}. The curves were shown in **Figure S10.**

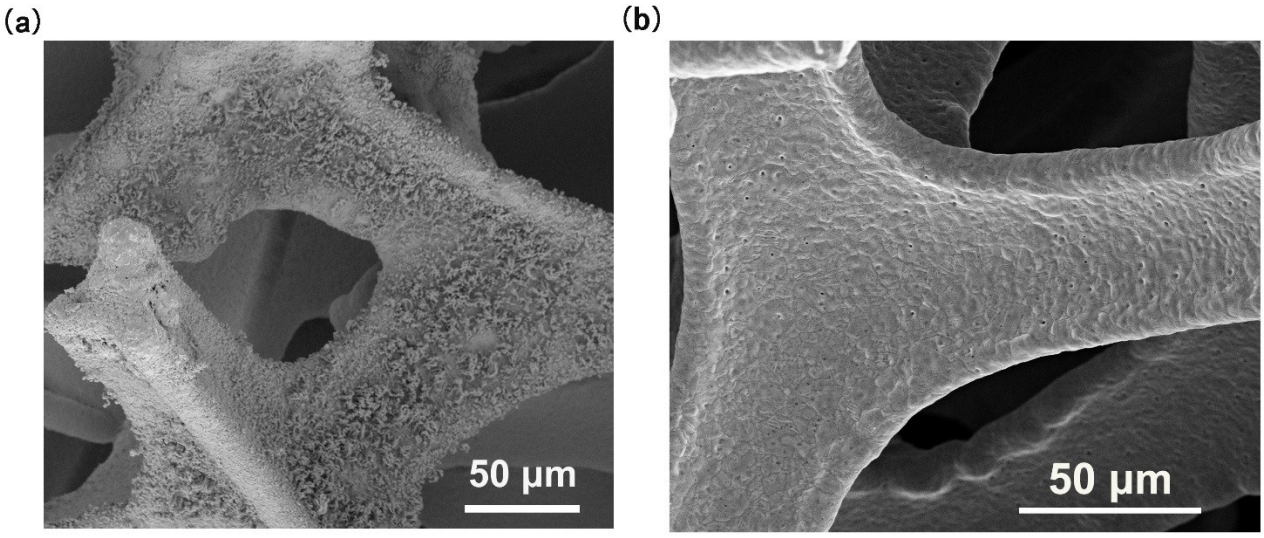

Figure S1. SEM images of **(a)** $CoS_2/Ni_3S_2/CoNiO_x$ and **(b)** bare CoNi foam

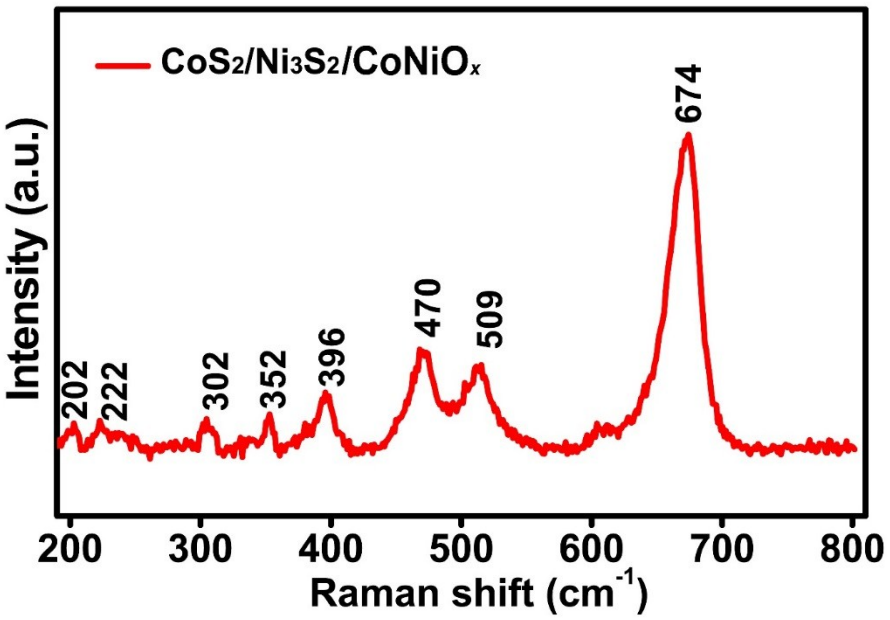

Figure S2. Raman spectrum of the as-prepared catalyst.

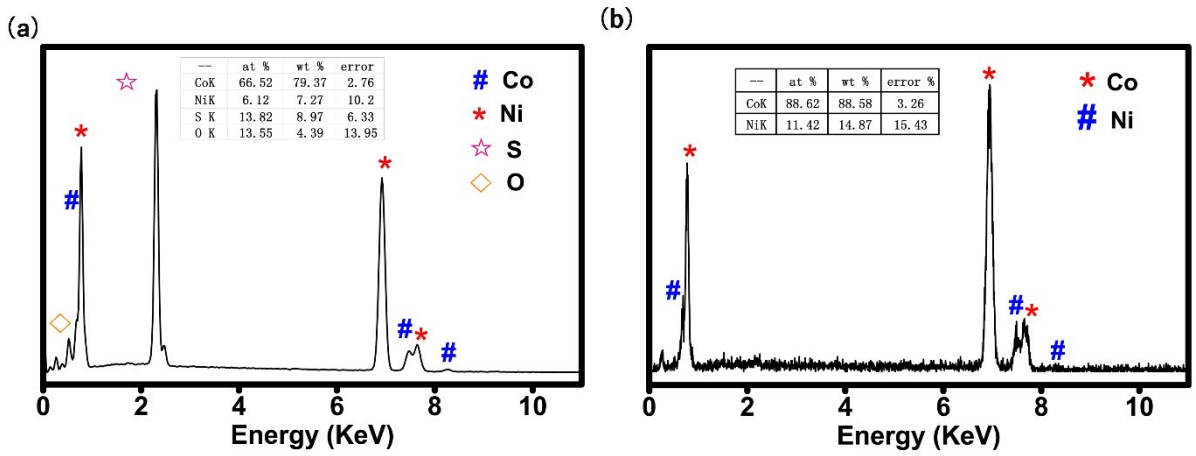

Figure S3. EDX spectra of **(a)** $CoS_2/Ni_3S_2/CoNiO_x$, **(b)** bare CoNi foam.

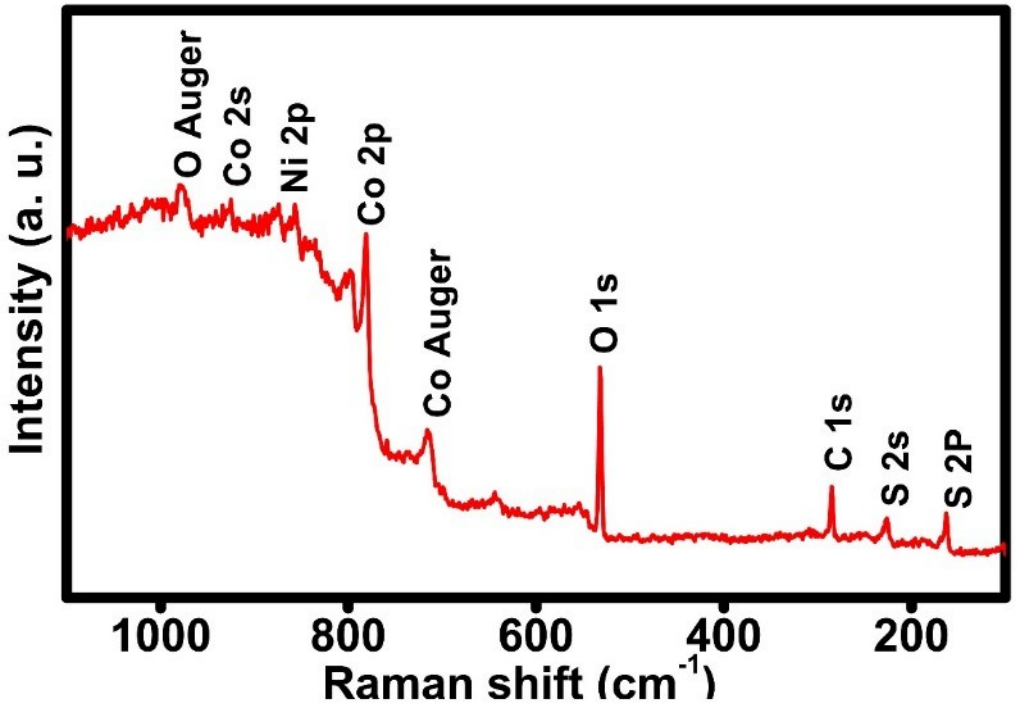

Figure S4. XPS survey of $CoS_2/Ni_3S_2/CoNiO_x$ catalyst.

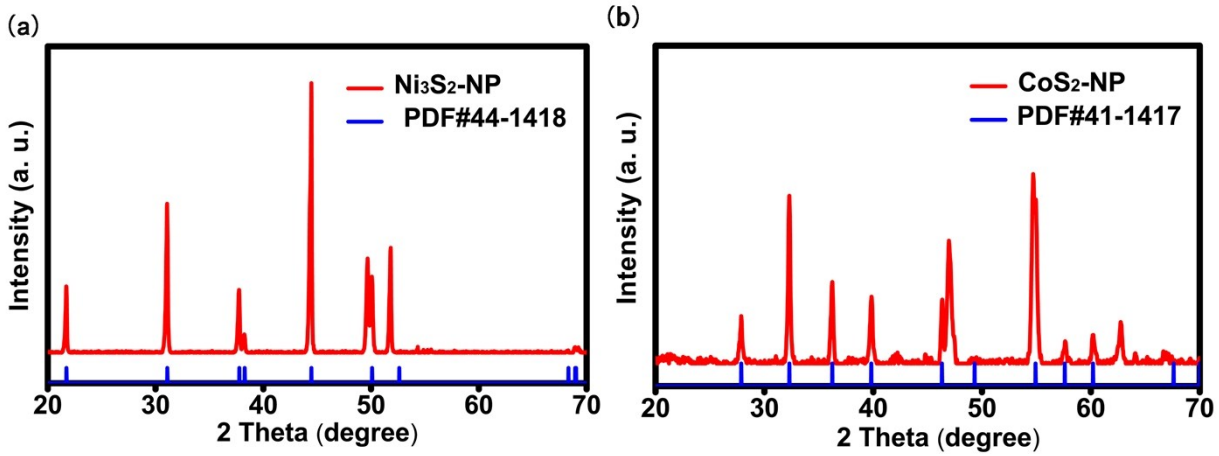

Figure S5. XRD patterns of **(a)** Ni_3S_2-NP, **(b)** CoS_2-NP.

XRD patterns of prepared Ni_3S_2-NP and CoS_2-NP were shown in **Figure S5**, suggesting that the diffraction peaks of catalyst match well with Ni_3S_2 (PDF#44-1418) and CoS_2 (PDF#41-1471).

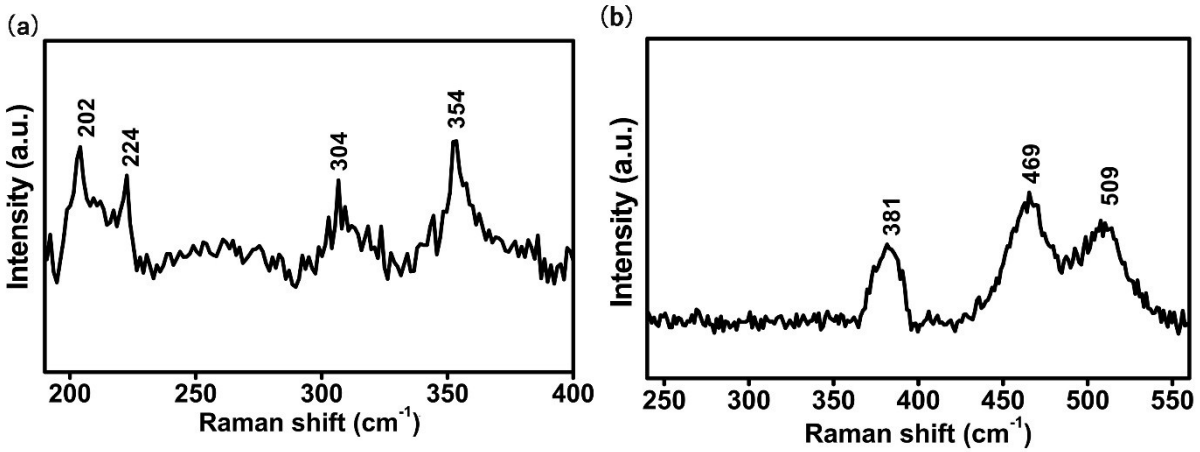

Figure S6. Raman spectra of **(a)** Ni_3S_2-NP, **(b)** CoS_2-NP.

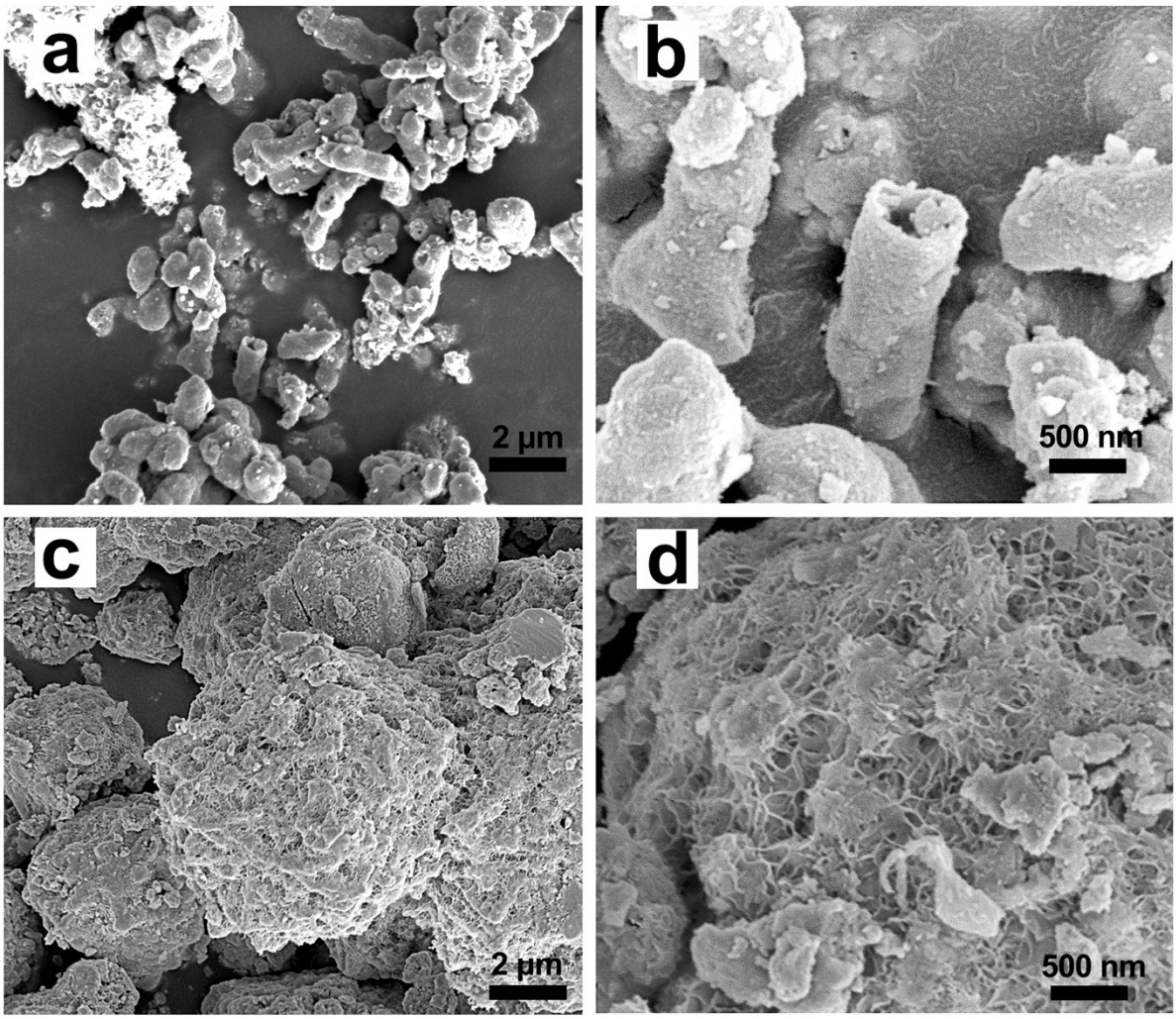

Figure S7. SEM images of **(a-b)** CoS_2-NP and **(c-d)** Ni_3S_2-NP.

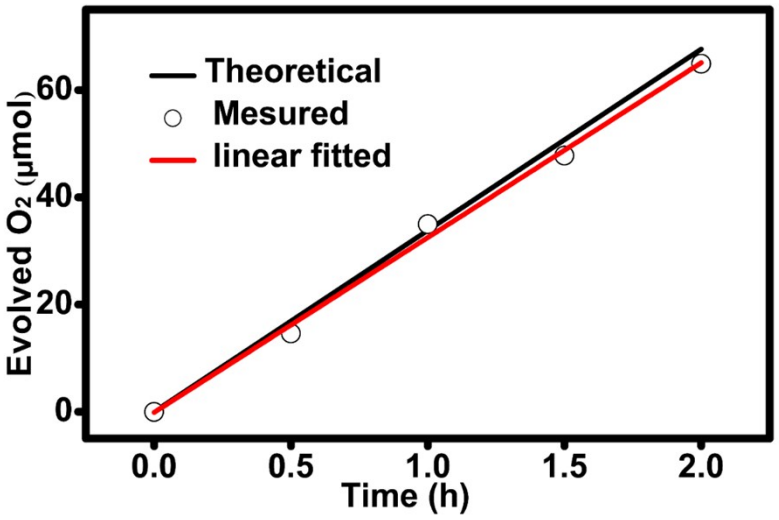

Figure S8. Determination of Faraday efficiency. Ring: measured data. Red line: linear fitting of measured data. Black line: Theoretical amount of oxygen as assumed by passed charge with 100% Faradaic efficiency.

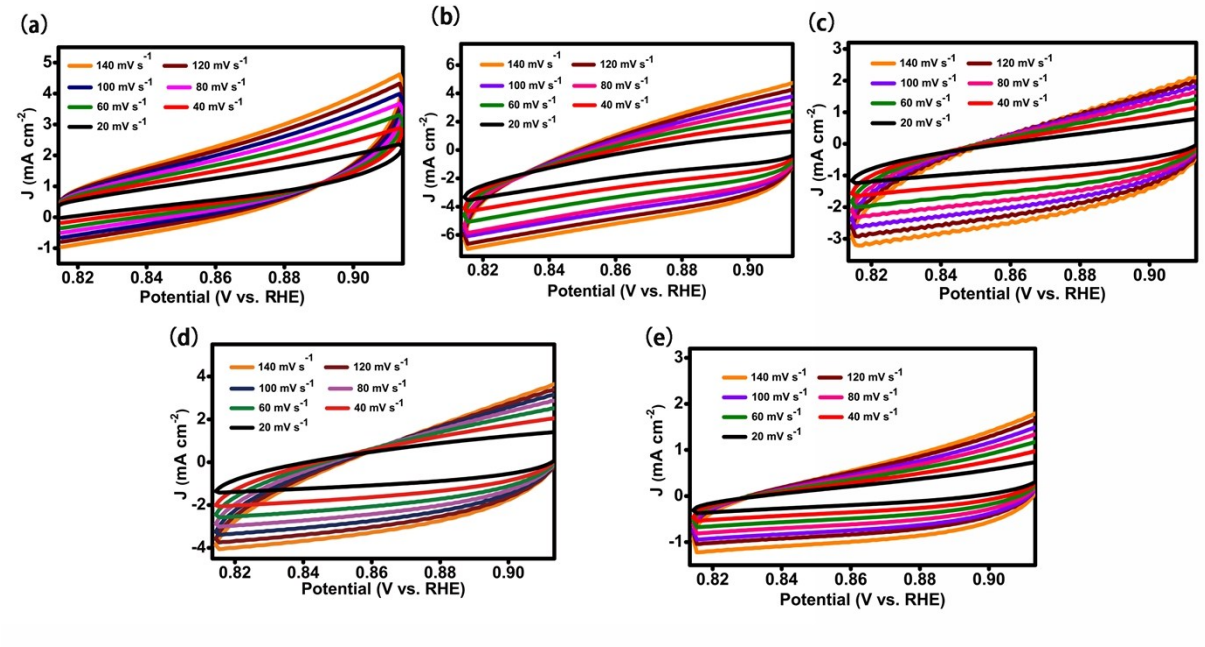

Figure S9. CV curves of **(a)** $CoS_2/Ni_3S_2/CoNiO_x$ catalyst, **(b)** RuO_2, **(c)** Ni_3S_2-NP, **(d)** CoS_2-NP, and **(e)** blank CoNi foam swept between 0.814 V ~ 0.914 V in 1.0 M KOH at seven different scan rates (20, 40, 60, 80, 100, 120, and 140 mV s^{-1}) for estimation of C_{dl}.

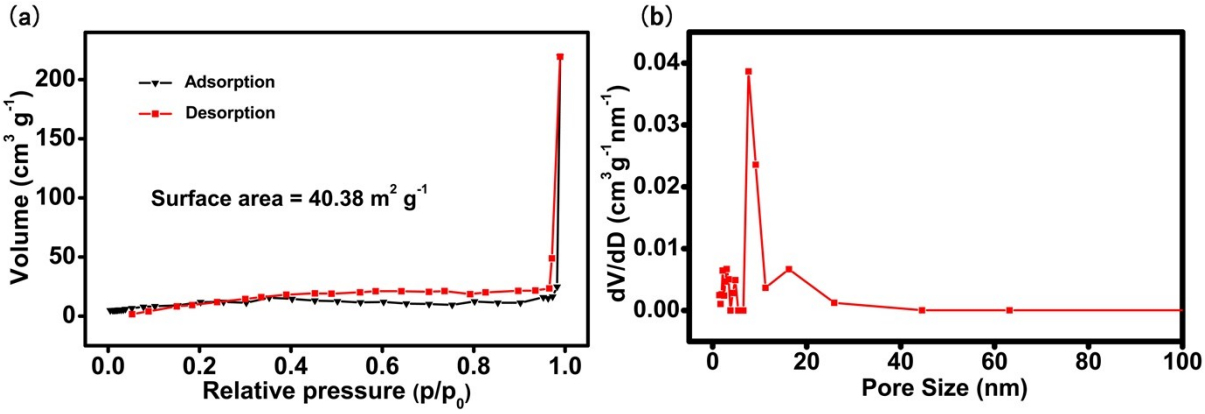

Figure S10. (a) N_2 adsorption-desorption isotherm and **(b)** BJH pore size distribution curve of the $CoS_2/Ni_3S_2/CoNiO_x$.

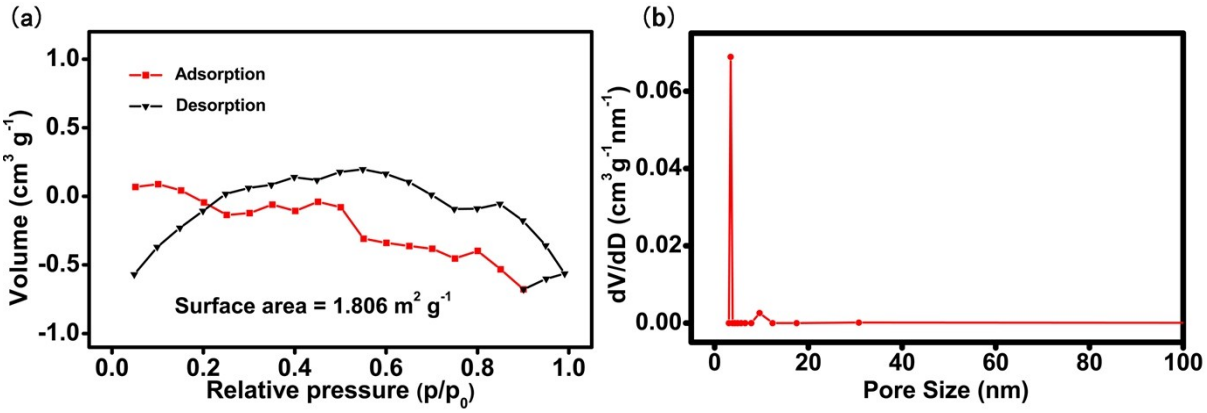

Figure S11. (a) N_2 adsorption-desorption isotherm and **(b)** BJH pore size distribution curve of the bare CoNi foam.

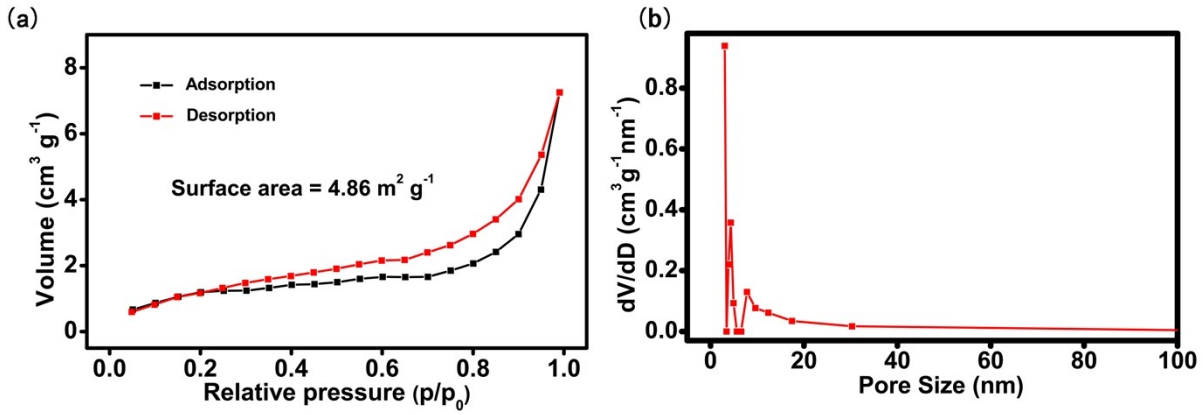

Figure S12. (a) N_2 adsorption-desorption isotherm and **(b)** BJH pore size distribution curve of the CoS_2-NP.

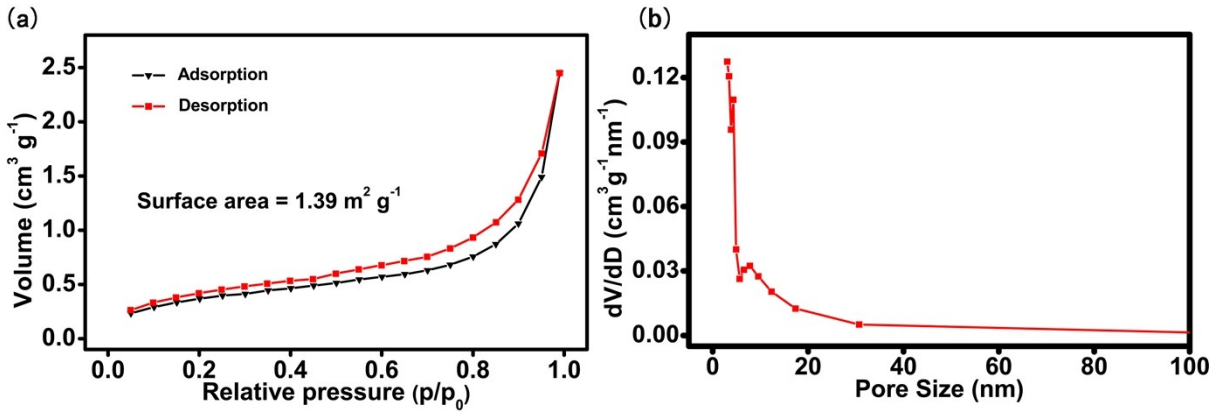

Figure S13. (a) N_2 adsorption-desorption isotherm and **(b)** BJH pore size distribution curve of the Ni_3S_2-NP.

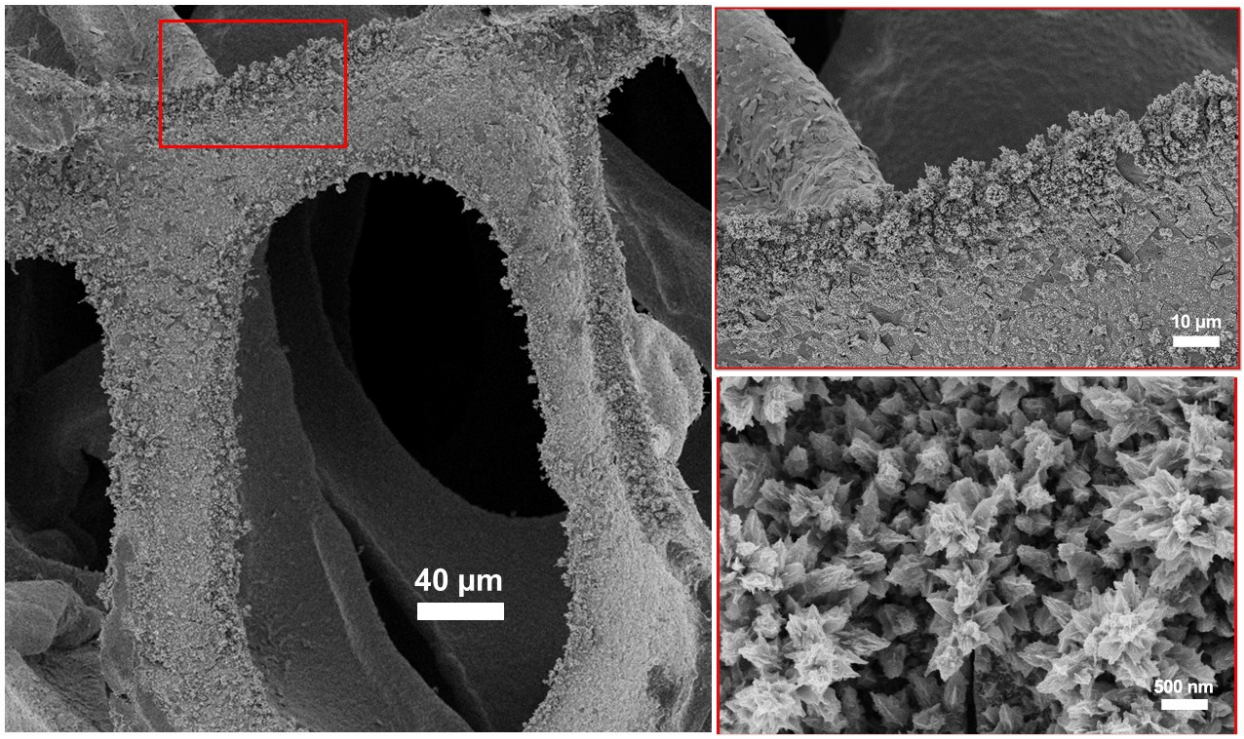

Figure S14. SEM image of the catalyst after the durability test at different magnification. **(a)** foam skeleton, **(b)** and **(c)** different magnification of red area.

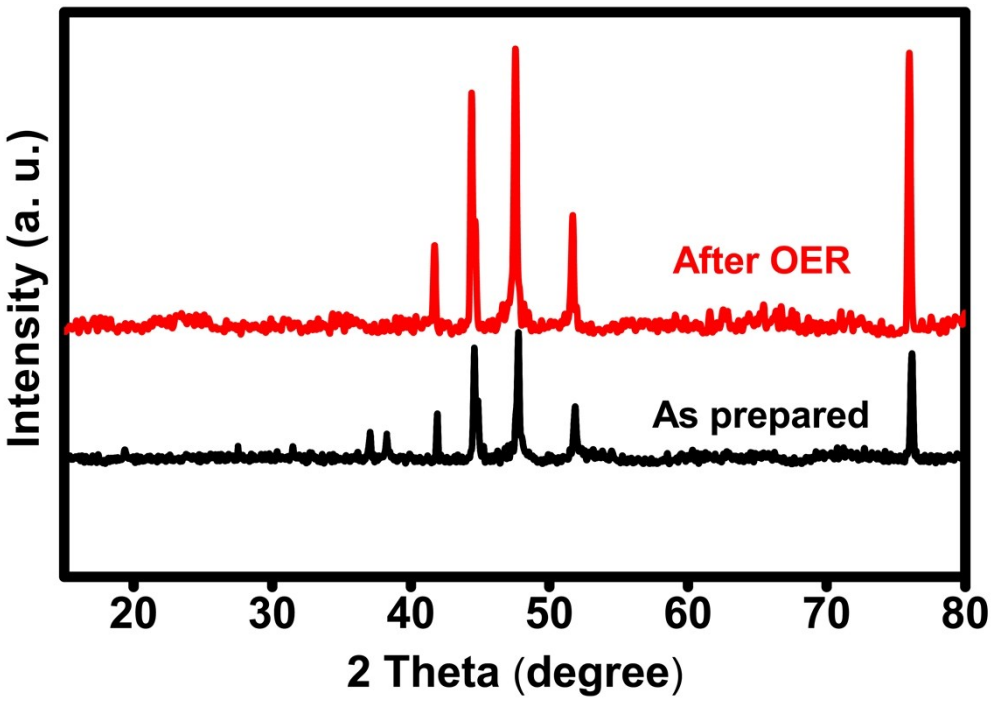

Figure S15. XRD patterns of post-catalyst (red), and the patterns of as-prepared catalyst (black) for comparison.

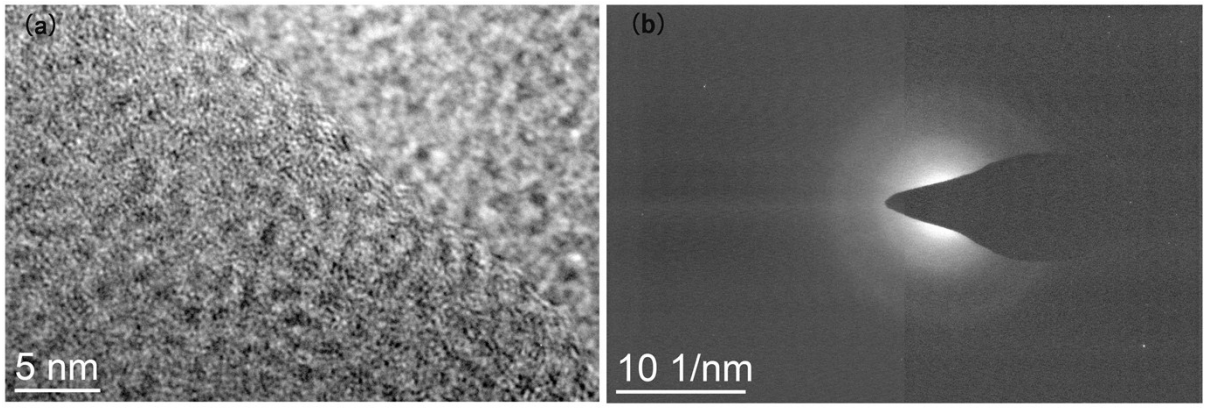

Figure S16. (a) HRTEM and **(b)** SAED patterns of the catalyst after OER.

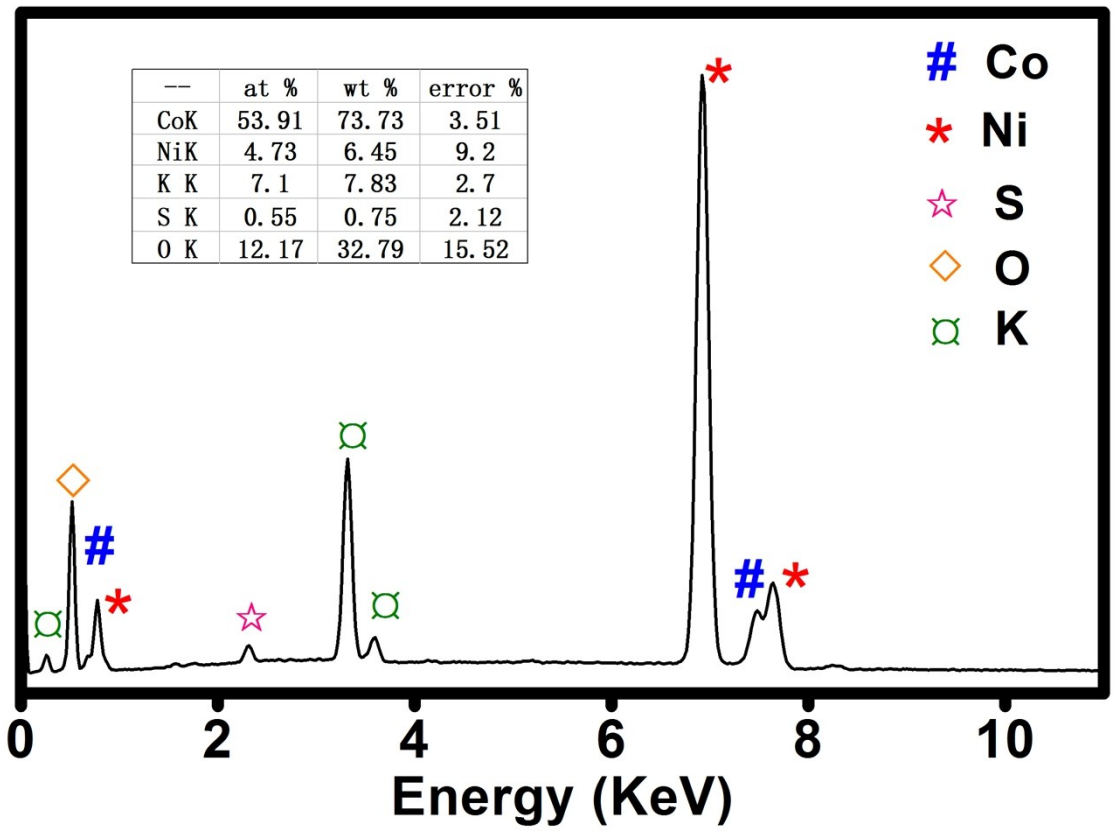

Figure S17. EDX spectrum of the catalyst after OER.

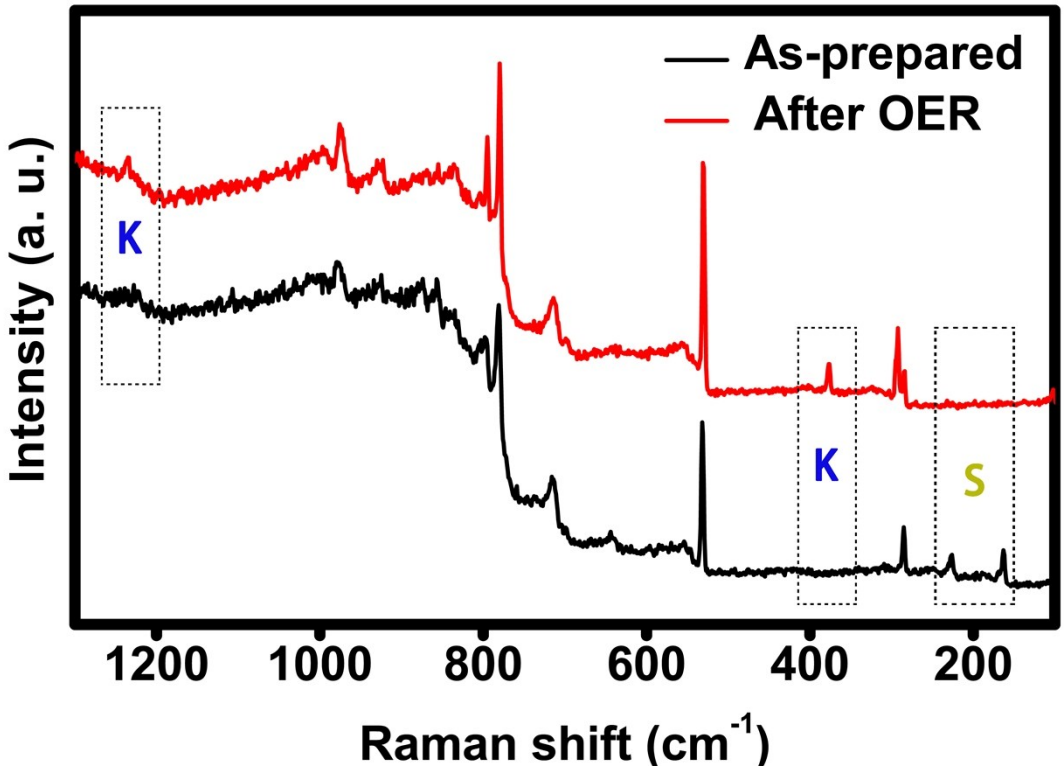

Figure S18. XPS survey of the catalyst after OER.

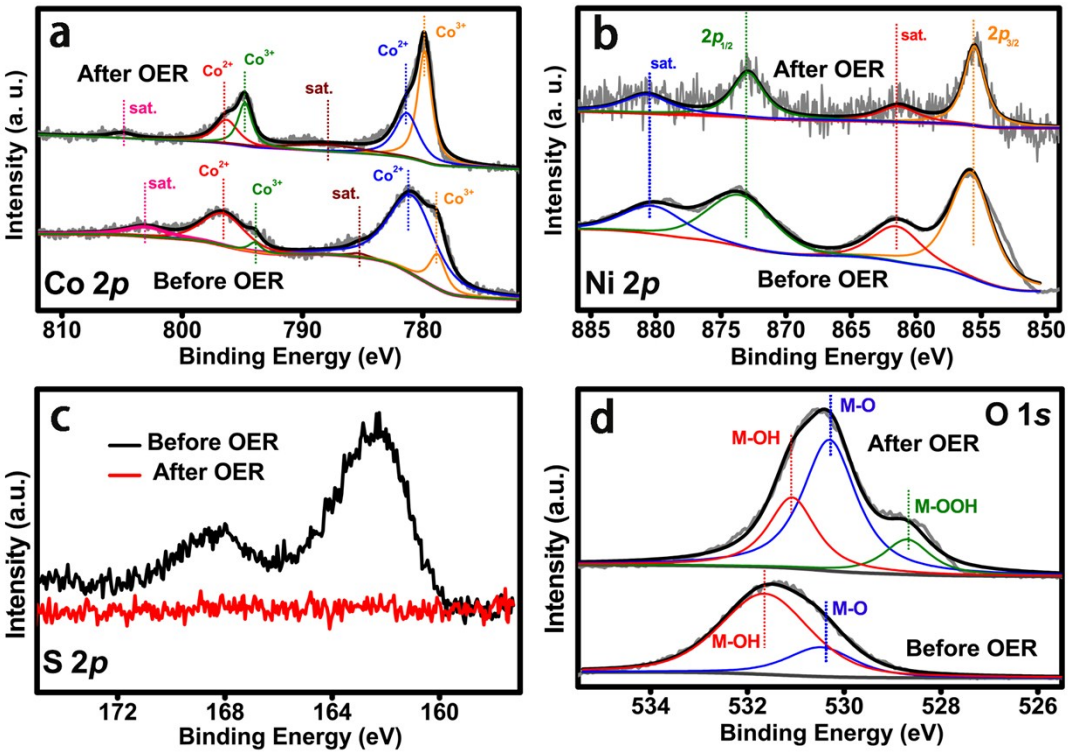

Figure S19. Sections of the XPS spectra of the catalyst before and after OER around the (a) Co 2*p*, (b) Ni 2*p*, (c) S 2*p* and (d) O 1*s* energy regions.

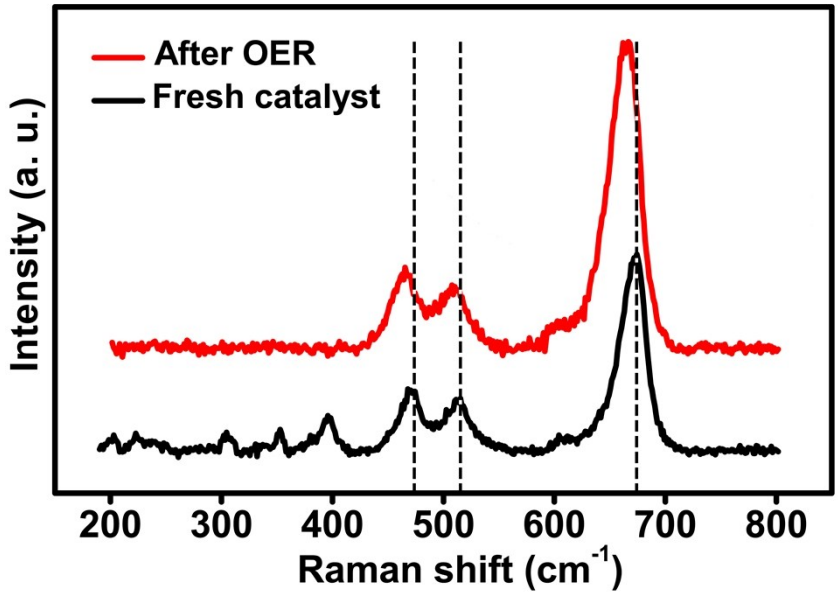

Figure S20. Raman spectra of the catalyst before (black) and after OER (red).

Table S1. Comparison of OER performance of CoNi-based electrocatalysts.

Electrodes and test conditions	Loading amount ($mg \cdot cm^{-2}$)	η_{10} (mV)	Tafel slope ($mV \cdot dec^{-1}$)	Stability	References
$CoS_2/Ni_3S_2/CoNiO_x$/CoNi foam, 1 M KOH	**~ 0.55**	**256 300 ((η_{100}))**	**43.4**	**1000 $mA \cdot cm^{-2}$, One week, 30% KOH, 25 mV potential increment**	**This work**
NiCoP/NF 1 M KOH	1.8	280	85	10 $mA \cdot cm^{-2}$, 24 h, 1 M KOH, No decay.	S1
NCO-HNSs on FTO, 1 M NaOH	1.6	280	87	η=370 mV, 18 h, 1 M KOH, 96% retention	S2
$NiCo_2O_4$ NA/CC, 1 M KOH	4	340 (η_{100})	89	20 $mA \cdot cm^{-2}$, 12 h, 1 M KOH, No decay.	S3
Core–Shell Ni-Co Nanowire/CF 1 M KOH	0.3	302	43.6	20 $mA \cdot cm^{-2}$, 10 h, 1 M KOH, 62% retention	S4
$(Ni_{0.33}Co_{0.67})S_2$ NW-CC, 1 M KOH	~ 3.5	295(η_{100})	78	η=275 mV, 24 h, 1 M KOH, 94% retention	S5
Co–Ni-Based Nanotubes/Cu foil, 1M KOH	-	280	77	η=320 mV, 24 h, 1 M KOH, 70% retention	S6
$NiCo_2O_4$ NWA /NF 1 M KOH	-	260	40.1	η=300 mV, 50 h, 1 M KOH, 85%	S7

				retention	
$Ni_{0.51}Co_{0.49}P$/NF, 1 M KOH	-	239	45	50 mA·cm^{-2}, 24 h, 1 M KOH, 97% retention	S8
Ternary NiCoP nanosheet, 1 M KOH	5	308	-	η=350 mV, 10 h, 1 M KOH, 97.8% retention	S9
Nest-like NiCoP/NF, 1 M KOH	~2	242 330 (η_{100})	64.2	50 mA·cm^{-2}, 11 h, 1 M KOH, almost no decay	S10
P‑Doped Co−Ni−S Nanosheets/NF, 1 M KOH	6.9	292 (η_{100})	61.1	10 mA·cm^{-2}, ~16 h, 1 M KOH, almost no decay	S11
$NiCo_2O_4$ Hollow Microcuboids/GC, 1 M NaOH	1	290	53	10 mA·cm^{-2}, ~32 h, 1 M NaOH, 10 mV increase of η	S12
$(Co_{1-x}Ni_x)(S_{1-y}P_y)_2$/Graphene/GC, 1 M NaOH	3	285	105	10 mA·cm^{-2}, ~32 h, 1 M NaOH, stable	S13
NiCo/$NiCo_2S_4$@NiCo/NF, 1 M NaOH	- (in situ)	294	59.6	η=280 mV, ~28 h, 1 M KOH, almost no decay	S14
NiCoP NR@NS/GC, 1 M NaOH	5	268	71	10 mA·cm^{-2}, 20 h, 1 M NaOH, a slight degradation	S15
$NiCo_2O_4$/NF, 1 M NaOH	7.5	~360	106	10 mA·cm^{-2}, 8 h 1 M KOH, almost no	S16

				decay	
$CoNi/CoFe_2O_4$ /NF, 1 M NaOH	2	230±2	45	100 mA·cm^{-2}, 48 h 1 M KOH, slight variation	S17
$CoNiPS_3$/C nanodots/GC, 1 M NaOH	~0.43	262 (η_{30})	56	η~ 250 mV, 22 h, 1 M KOH, no decay	S18
Au-doped Co/Ni-Hydroxide/GC	-	340	40	5 mA·cm^{-2}, 24 h, 1 M NaOH, stable	S19
Fe doped Co-Ni oxide	0.12	336	36	10 mA·cm^{-2}, 14 h, 1 M NaOH, stable	S20
Ni-Co-B	4	300	113	40 mA·cm^{-2}, 55 h, 1 M KOH, little aggregation	S21
NCO/G NSs @ GC	0.13	400 (η_{100})	65.9	1.61 V vs. RHE, 20 h 1 M KOH, no decay	S22

NCO-HNS: Ni–Co oxide hierarchical nanosheets;

FTO: Fluorine-doped tin oxide;

NA: Nanoarray;

CC: Carbon cloth;

NWA: Nanowire array;

NF: Ni foam;

NF: Ni foam;

NCO/G NS: Ni–Co oxide graphene nanosheets;

Reference

[S1] Liang H., Gandi A. N., Anjum D. H., Wang X., Schwingenschlögl U., Alshareef H. N., Plasma-Assisted Synthesis of NiCoP for Efficient Overall Water Splitting. *Nano Lett.* **2016**, 16, 7718−7725.

[S2] Wang H.-Y., Hsu Y.-Y., Chen R., Chan T.-S., Chen H. M., Liu B., Ni^{3+}-Induced Formation of Active NiOOH on the Spinel Ni-Co Oxide Surface for Efficient Oxygen Evolution Reaction. *Adv. Energy Mater.* **2015,** 5, 1500091.

[S3] Liu D., Lu Q., Luo Y., Sun X., Asiri A. M., $NiCo_2S_4$ nanowires array as an efficient bifunctional electrocatalyst for full water splitting with superior activity. *Nanoscale* **2015**, 7, 15122−15126.

[S4] Bae S.-H., Kim J.-E., Randriamahazaka H., Moon S.-Y., Park J.-Y., Oh I.-K., Seamlessly Conductive 3D Nanoarchitecture of Core–Shell Ni-Co Nanowire Network for Highly Efficient Oxygen Evolution. *Adv. Energy Mater.* **2016**, 1601492.

[S5] Zhang Q., Ye C., L. L. Xiao, Deng Y. H., Tao B. X., Xiao W., Li L. J., Li N. B., Luo H. Q., Self-Interconnected Porous Networks of NiCo Disulfide as Efficient Bifunctional Electrocatalysts for Overall Water Splitting, *ACS Appl. Mater. Inter.* **2018**, 10, 27723−27733.

[S6] Li S., Wang Y., Peng S., Zhang L., Al-Enizi A.M., Zhang H., Sun X., Zheng G., Co–Ni-Based Nanotubes/Nanosheets as Efficient Water Splitting Electrocatalysts. *Adv. Energy Mater.* **2016**, 6, 1501661.

[S7] Sivanantham A., Ganesan P., Shanmugam S., Hierarchical $NiCo_2S_4$ Nanowire Arrays Supported on Ni Foam: An Efficient and Durable Bifunctional Electrocatalyst for Oxygen and Hydrogen Evolution Reactions. *Adv. Funct. Mater.* **2016**, 26, 4661−4672.

[S8] Yu J., Li Q., Li Y., Xu C.-Y., Zhen L., Dravid V. P., Wu J., Ternary Metal Phosphide with Triple-Layered Structure as a Low-Cost and Efficient Electrocatalyst for Bifunctional Water Splitting. *Adv. Funct. Mater.* **2016**, 26, 7644−7651.

[S9] Li Y., Zhang H., Jiang M., Sun X., Duan X., Ternary NiCoP nanosheet arrays: An excellent bifunctional catalyst for alkaline overall water splitting. *Nano Res.* **2016**, 9, 2251–2259.

[S10] Du C., Yang L., Yang F., Cheng G. Luo W., Nest-like NiCoP for Highly Efficient Overall Water Splitting. *ACS Catal.* **2017**, 7, 4131−4137.

[S11] Zhang F., Ge Y., Chu H., Dong P., Baines R., Pei Y., Ye M., Shen J., Dual-Functional Starfish-like P‑Doped Co-Ni-S Nanosheets Supported on Nickel Foams with Enhanced Electrochemical Performance

and Excellent Stability for Overall Water Splitting. *ACS Appl. Mater. Inter.* **2018**, 10, 7087−7095.

[S12] Gao X., Zhang H., Li Q., Yu X., Hong Z., Zhang X., Liang C., Lin Z., Hierarchical $NiCo_2O_4$ Hollow Microcuboids as Bifunctional Electrocatalysts for Overall Water-Splitting., *Angew. Chem. Int. Ed.* **2016**, 55, 6290−6294.

[S13] Song H. J., Yoon H., Ju B., Lee G.-H., Kim D.-W., 3D Architectures of Quaternary Co-Ni-S-P/Graphene Hybrids as Highly Active and Stable Bifunctional Electrocatalysts for Overall Water Splitting., *Adv. Energy Mater*. **2018**, 8, 1802319.

[S14] Ning Y., Ma D., Shen Y., Wang F., Zhang X., Constructing hierarchical mushroom-like bifunctional NiCo/$NiCo_2S_4$@NiCo/Ni foam electrocatalysts for efficient overall water splitting in alkaline media., *Electrochim. Acta.*, 2018, 265, 19−31.

[S15] Wang J.-G., Hua W., Li M., Liu H., Shao M., Wei B., Structurally Engineered Hyperbranched NiCoP Arrays with Superior Electrocatalytic Activities toward Highly Efficient Overall Water Splitting., *ACS Appl. Mater. Interfaces.*, 2018, DOI: 10.1021/acsami.8b11576.

[S16] Yang L., Zhang B., Fang B., Feng L., A comparative study of $NiCo_2O_4$ catalyst supported on Ni foam and from solution residuals fabricated by a hydrothermal approach for electrochemical oxygen evolution reaction., *Chem. Commun.*, **2018**, 54, 13151−13154.

[S17] Li S., Sirisomboonchai S., Yoshida A., An X., Hao X., Abudul A., Guan G., Bifunctional CoNi/$CoFe_2O_4$ /Ni foam electrodes for efficient overall water splitting at a high current density, *J. Mater. Chem. A*, **2018**, 6, 19221–19230.

[S18] Liang Q., Zhong L., Du C., Zheng Y., Luo Y., Xu J., Li S., Yan Q., Mosaic-Structured Cobalt Nickel Thiophosphate Nanosheets Incorporated N-doped Carbon for Efficient and Stable Electrocatalytic Water Splitting. *Adv. Funct. Mater.* **2018**, 28, 1805075.

[S19] Sultana U. K., Riches J. D., O'Mullane A. P., Gold Doping in a Layered Co-Ni Hydroxide System via Galvanic Replacement for Overall Electrochemical Water Splitting. *Adv. Funct. Mater.* **2018**, 28, 1804361.

[S20] Deng X., Öztürk S., Weidenthaler C., Tüysüz H., Iron-Induced Activation of Ordered Mesoporous Nickel Cobalt Oxide Electrocatalyst for the Oxygen Evolution Reaction, *ACS Appl. Mater. Interfaces* **2017**, 9, 21225−21233.

[S21] Wang S., He P., Xie Z., Jia L., He M., Zhang X., Dong F., Liu H., Zhang Y., Li C., Tunable nanocotton-like amorphous ternary Ni-Co-B: A highly efficient catalyst for enhanced oxygen evolution reaction. *Electrochimica Acta*, **2019**, 296, 644–652.

[S22] Tian J., Chen Jie, Liu J., Tian Q., Chen P., Graphene quantum dot engineered nickel-cobalt phosphide as highly efficient bifunctional catalyst for overall water splitting. *Nano Energy* **2018**, 48, 284–291.